NUCLEAR THEORY, Vol. 31 (2012)
eds. A. Georgieva, N. Minkov, Heron Press, Sofia

Description of Non-Yrast Split Parity-Doublet Bands in Odd-*A* Nuclei

N. Minkov[1,2], **S. Drenska**[1], **K. Drumev**[1], **M. Strecker**[2], **H. Lenske**[2], **W. Scheid**[2]

[1]Institute of Nuclear Research and Nuclear Energy, Bulgarian Academy of Sciences, Tzarigrad Road 72, BG-1784 Sofia, Bulgaria

[2]Institut für Theoretische Physik der Justus-Liebig-Universität, Heinrich-Buff-Ring 16, D–35392 Giessen, Germany

Abstract.

The model of coherent quadrupole and octupole motion (CQOM) is applied to describe non-yrast split parity-doublet spectra in odd-mass nuclei. The yrast levels are described as low-energy rotation-vibration modes coupled to the ground single-particle state, while the non-yrast parity-doublet structures are obtained as higher-energy rotation-vibration modes. It is shown that the extended model scheme describes both the yrast and non-yrast quasi-parity doublet spectra and the related B(E1) and B(E2) transition rates in different regions of heavy odd-A nuclei. The involvement of the reflection-asymmetric deformed shell model to describe the single-particle motion and the Coriolis interaction on a deeper level is discussed.

1 Introduction

The observation of quasi parity-doublet spectra in odd mass nuclei is usually related to the presence of quadrupole-octupole deformations [1]. The low-lying (yrast) structure of the octupole spectra was relatively well studied and described within various collective and microscopic model approaches (see [1,2] and references therein), while the interpretation and the model classification of the higher, non-yrast, parts of these spectra is still quite limited. Recently the model of Coherent Quadrupole-Octupole Motion (CQOM) [3, 4] has been applied to non-yrast alternating-parity bands and the attendant B(E1), B(E2) and B(E3) transition probabilities in even-even nuclei showing that the octupole degrees of freedom have a persistent role in the higher energy part of the spectrum [5].

The purpose of the present work is to show that the model scheme is also capable to describe non-yrast quadrupole-octupole excitations in odd-mass nuclei by extending the original consideration proposed in [4]. For this reason it is assumed that the non-yrast parity-doublet spectra can be associated to essentially collective rotation-vibration degrees of freedom. The coupling of the core to the odd nucleon and the Coriolis interaction are taken into account phenomeno-

logically. The model approach remains open for a microscopic treatment of the single-particle degrees of freedom.

In Section 2 the CQOM model formalism for the split-parity doublet spectra is briefly presented. In Section 3 numerical results and a discussion on the application of the model to a number of odd-mass nuclei in the rare-earth and actinide region are presented. In Section 4 concluding remarks are given.

2 Model of Coherent Quadrupole–Octupole Motion

The model Hamiltonian for odd-mass nuclei can be taken as [4]

$$H_{qo} = -\frac{\hbar^2}{2B_2}\frac{\partial^2}{\partial\beta_2^2} - \frac{\hbar^2}{2B_3}\frac{\partial^2}{\partial\beta_3^2} + \frac{1}{2}C_2{\beta_2}^2 + \frac{1}{2}C_3{\beta_3}^2 + \frac{X(I,K)}{d_2\beta_2^2 + d_3\beta_3^2} \quad (1)$$

where β_2 and β_3 are axial quadrupole and octupole variables, respectively, and B_2 (B_3), C_2 (C_3) and d_2 (d_3) are quadrupole (octupole) mass, stiffness and inertia parameters, respectively. The quantity

$$X(I,K) = \frac{1}{2}\left[d_0 + I(I+1) - K^2 + \pi a \delta_{K,\frac{1}{2}}(-1)^{I+1/2}\left(I+\frac{1}{2}\right)\right] , \quad (2)$$

involves the collective angular momentum I, its third projection K and the decoupling factor a for the intrinsic states with $K = 1/2$. The parameter d_0 determines the potential core at $I = 0$. In the present work the decoupling factor is considered as a model parameter adjusted to the experimental data. In [6] we show that to treat the Coriolis interaction in CQOM microscopically, one can apply an appropriate parity-projection particle-core coupling scheme in which the decoupling factor is calculated by using a reflection-asymmetric deformed shell model.

Under the assumption of coherent quadrupole-octupole oscillations with a frequency $\omega = \sqrt{C_2/B_2} = \sqrt{C_3/B_3} \equiv \sqrt{C/B}$, and after introducing ellipsoidal coordinates $\beta_2 = p\eta\cos\phi$, $\beta_3 = q\eta\sin\phi$, with $p = \sqrt{d/d_2}$, $q = \sqrt{d/d_3}$ and $d = (d_2 + d_3)/2$, the collective energy of the system is obtained in the form [3, 4]

$$E_{nk}(I) = \hbar\omega\left[2n + 1 + \sqrt{k^2 + bX}\right] , \; n = 0, 1, 2, ...; \; k = 1, 2, 3, ..., \quad (3)$$

where $b = 2B/(\hbar^2 d)$. The quadrupole-octupole vibration wave function is

$$\Phi^{\pi}_{nkI}(\eta,\phi) = \psi^I_{nk}(\eta)\varphi^{\pi}_k(\phi), \quad (4)$$

where the "radial" part $\psi^I_{nk}(\eta)$ involves generalized Laguerre polynomials in the variable η [3], while the "angular" part in the variable ϕ appears with a positive or negative parity, $\pi_\varphi = \pm$, as follows

$$\varphi^+_k(\phi) = \sqrt{2/\pi}\cos(k\phi) , \qquad k = 1, 3, 5, ... , \quad (5)$$

$$\varphi^-_k(\phi) = \sqrt{2/\pi}\sin(k\phi) , \qquad k = 2, 4, 6, ... \quad (6)$$

The total core+particle wave function for a state with angular momentum I^π belonging to a parity-doublet sequence in odd-even nuclei is given by [4]

$$\begin{aligned}\Psi^{\pi}_{nkIMK}(\eta,\phi) &= \sqrt{\frac{2I+1}{16\pi^2}}\Phi^{\pi}_{nkI}(\eta,\phi)\left[D^{I}_{M\,K}(\theta)\mathcal{F}_K\right. \\ &+ \left.\pi\pi_{\rm sp}(-1)^{I+K}D^{I}_{M\,-K}(\theta)\mathcal{F}_{-K}\right]\ , \end{aligned} \tag{7}$$

where $\mathcal{F}_K$ and $\pi_{\rm sp}$ are the wave function and the parity of the single-particle state, respectively.

The energy spectrum is determined in (3) by the quantum numbers n and k. The parity-doublet structure is imposed by the condition $\pi = \pi_\varphi \cdot \pi_{\rm sp}$. The parity doublet (a couple of states with the same angular momentum $I^\pm$ and opposite parities) is determined by a given n and a pair of odd and even k-values, $k_n^{(+)}$ and $k_n^{(-)}$ ($k_n^{(+)} < k_n^{(-)}$). The k-values are determined so that $k = k_n^{(+)}$ for $I^{\pi=\pi_{\rm sp}}$ and $k = k_n^{(-)}$ for $I^{\pi=-\pi_{\rm sp}}$. The difference between $k_n^{(+)}$ and $k_n^{(-)}$ generates the splitting of the parity-doublet. The yrast doublet is formed above the ground state whose parity is $\pi_{\rm sp}^{(0)}$. The non-yrast doublets are coupled to excited s.p. or quasi-particle (q.p.) states (if the pairing correlations are taken into account) whose parity $\pi_{\rm sp}^{(n)}$ determines the doublet structure, with the $k_n^{(+)}$ and $k_n^{(-)}$ accordance, as in the case of the ground-state (yrast) doublet. The index n also labels the different intrinsic configurations to which the non-yrast doublets are coupled.

By using the wave functions (7) one can calculate B(E1), B(E2) and B(E3) transition probabilities in the yrast and non-yrast quasi-doublet spectra. The relevant formalism was originally developed in [3, 4] and further extended to the non-yrast alternating-parity states of even-even nuclei [5]. In the present work we apply the same formalism as extended in [5]. The only difference is in the Clebsch-Gordan coefficients which now involve the quantum numbers K_i and K_f of the initial and final states. Then the reduced electric transition probabilities with multipolarity $\lambda = 1, 2, 3$ are taken as

$$\begin{aligned}B(E\lambda; n_i k_i I_i K_i \to n_f k_f I_f K_f) &= \frac{2\lambda+1}{4\pi(4-3\delta_{\lambda,1})}\langle I_i K_i \lambda 0 | I_f K_f\rangle^2 \\ &\times\ R^2_\lambda(n_i k_i I_i \to n_f k_f I_f),\end{aligned} \tag{8}$$

where the factors R_λ involve integrals over the radial η and and the angular ϕ variables (see [5] for details). Due to the imposed axial symmetry the B(Eλ) probabilities (8) are non-zero only between states with the same K-values ($K_i = K_f$). Therefore, in the present work we only consider transitions connecting states with the same K. The consideration of transitions with $K_i \neq K_f$ can be implemented after taking a more general transition operator in Eq. (19) of [5] involving $\sum_\nu D^\lambda_{\mu,\nu}$ and also by taking into account the Coriolis K-mixing effect in the s.p. states. This is the subject of further work.

We remark that the ground state, the excited q.p. states, the respective decoupling factors (in case of $K = 1/2$), as well as the Coriolis mixing contributions can also be obtained through a reflection-asymmetric deformed shell model (DSM). This possibility provides a natural way to connect the collective CQOM model with the microscopic approach. Although the work in this direction is in an essential progress, here we consider the s.p. degree of freedom phenomenologically. Thus for a given doublet we take the s.p. parity and the K value as suggested by the experimental analysis and by microscopic calculations reported in the literature. On the other hand the doublet band-heads are obtained as different rotation-vibration modes characterized by the CQOM oscillator quantum number $n = 0, 1, 2, ...$, and the respective decoupling factors a_n entering the expression (2) (in case of $K = 1/2$) which are adjusted according to the experimental data. It should be noted that these phenomenological decoupling factors are of great importance to determine the physically reasonable deformation regions [6] where the DSM calculations have to be performed after inserting the microscopic part in the CQOM.

3 Numerical results and discussion

In this section results of the CQOM model application to several odd-mass nuclei are presented. The model energy levels are determined by Eq. (3) as $\tilde{E}_{nk}(I) = E_{nk}(I) - E_{0k_{gs}}(I_{gs})$, where I_{gs} and k_{gs} are the angular momentum and k-values of the ground state, respectively. The model parameters ω, b and d_0 determine the energy levels, while the parameters $c = \sqrt{BC}/\hbar$ (see Eq. (13) in [5]), p (see Eqs (6), (36)-(38) in [5]) and e^1_{eff} (see the text after Eq. (23) in [5]) determine the transition probabilities. (See [5] for more details on the calculation of transition probabilities.) All these parameters are adjusted by simultaneously taking into account experimental data on the energy bands [7] and the available B(E1) and B(E2) transition probabilities [8]. In the cases of $K = 1/2$ bandheads the decoupling factor a_n is also adjusted. For each nucleus the calculations are performed on a net over the values of $k_n^{(+)}$ and $k_n^{(-)}$ providing the sets of k-values for the best description. Calculations have been performed for the nuclei ^{151}Pm, ^{155}Eu, ^{161}Dy, ^{157}Gd, ^{221}Fr, ^{223}Ra, ^{239}Pu, ^{239}Np and ^{243}Am in which both non-yrast parity-doublet levels and a number of B(E1) and B(E2) transition probabilities are observed.

The theoretical and experimental energy levels of the nuclei ^{155}Eu, ^{157}Gd, ^{161}Dy, ^{221}Fr, ^{223}Ra and ^{239}Pu are compared in Figures 1-4. The obtained parameter values and k-numbers are also given there. The respective transition probabilities are given in Table 1. In Figure 5 both, the energy levels and transition probabilities for the nuclei ^{239}Np and ^{243}Am are given. We see that for all considered nuclei the model suggests the existence of at least one excited non-yrast quasi parity-doublet band. In the nuclei ^{161}Dy and ^{239}Pu we also observe a second non-yrast doublet structure. In all considered nuclei the theoretical energy sequences reproduce the structure of the experimentally observed

bands. It is noticeable that in ^{239}Pu, Figure 4, the non-yrast levels are described together with the yrast band which expands to a very high angular momentum $I = 55/2$. At the same time the Coriolis decoupling in the yrast band and the second non-yrast band is also taken into account. Thus, the strong Coriolis decoupling observed in the nuclei ^{221}Fr and ^{223}Ra is described (see Figure 3). As a result the overall effect of the interchange of neighbouring angular momenta in the yrast levels of ^{221}Fr and in the second non-yrast sequence in ^{223}Ra due to the strong decoupling is reproduced. The obtained values of the decoupling

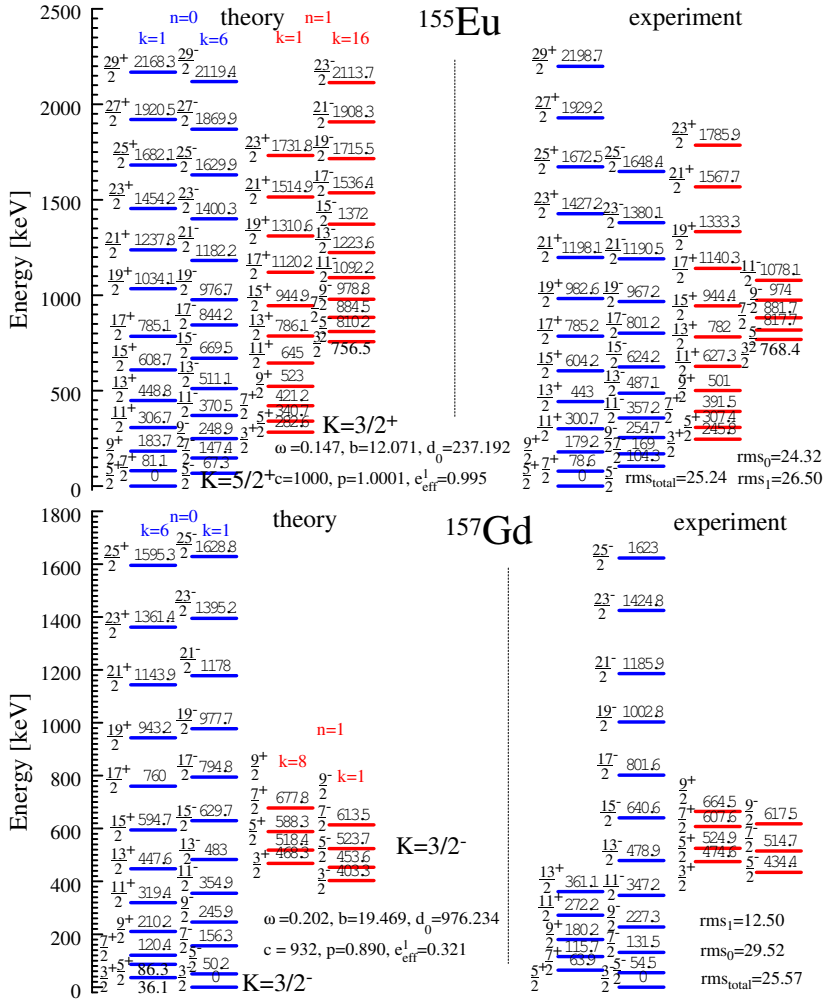

Figure 1. Theoretical and experimental parity-doublet levels for ^{155}Eu and ^{157}Gd. The root mean square (rms) factors are given in keV. Data from [7].

Table 1. Theoretical and experimental values of B(E1) and B(E2) transition probabilities in Weisskopf units (W.u.) for quasi parity-doublet spectra of several odd-mass nuclei. Notations: $I^{\pi_i}_{n_i} \to I^{\pi_f}_{n_f}$ with n_i and n_f denoting the doublet ($n = 0, 1, 2$). The data are taken from [8]. The uncertainties (in parentheses) refer to the last significant digits in the experimental data.

Mult	Transition	Th [W.u.]	Exp [W.u.]
		^{155}Eu	
E1	$5/2^-_0 \to 5/2^+_0$	0.00156	0.00156(19)
E1	$5/2^-_0 \to 7/2^+_0$	0.00063	0.00063(13)
		^{157}Gd	
E1	$5/2^+_0 \to 5/2^-_0$	5.21×10^{-6}	10.3×10^{-6} (22)
E1	$5/2^+_0 \to 3/2^-_0$	53.9×10^{-7}	4.6×10^{-7} (8)
E2	$5/2^-_0 \to 3/2^-_0$	311	293
E2	$7/2^-_0 \to 5/2^-_0$	195	230
E2	$7/2^-_0 \to 3/2^-_0$	130	119
		^{161}Dy	
E1	$5/2^-_0 \to 5/2^+_0$	0.000134	0.000139(4)
E1	$7/2^+_0 \to 5/2^-_0$	0.00004	0.0014 (6)
E1	$7/2^-_0 \to 7/2^+_0$	7.6×10^{-5}	5.5×10^{-5}(11)
E1	$7/2^-_0 \to 5/2^+_0$	4.0×10^{-5}	6.1×10^{-5} (6)
E2	$7/2^-_0 \to 5/2^-_0$	57	340 (10)
E2	$7/2^+_0 \to 5/2^+_0$	276	330 (10)
E2	$9/2^+_0 \to 7/2^+_0$	236	260(10)
E2	$11/2^+_0 \to 9/2^+_0$	184	160(10)
E2	$13/2^+_0 \to 11/2^+_0$	144	70 (3)
E2	$15/2^+_0 \to 13/2^+_0$	115	90 (3)
E2	$17/2^+_0 \to 15/2^+_0$	94	9 (8)
E2	$19/2^+_0 \to 17/2^+_0$	79	54 (16)
E2	$21/2^+_0 \to 19/2^+_0$	67	9 (8)
E2	$23/2^+_0 \to 21/2^+_0$	58	12 (8)
E2	$25/2^+_0 \to 23/2^+_0$	50	4 (9,-4)
E2	$9/2^+_0 \to 5/2^+_0$	77	94(10)
E2	$11/2^+_0 \to 7/2^+_0$	132	135 (25)
E2	$13/2^+_0 \to 9/2^+_0$	170	159(22)
E2	$15/2^+_0 \to 11/2^+_0$	197	190(3)
E2	$17/2^+_0 \to 13/2^+_0$	218	222 (21)
E2	$19/2^+_0 \to 15/2^+_0$	235	177 (9)
E2	$21/2^+_0 \to 17/2^+_0$	250	260 (3)
E2	$23/2^+_0 \to 19/2^+_0$	263	240 (3)
E2	$25/2^+_0 \to 21/2^+_0$	275	340 (7)
E2	$5/2^-_1 \to 3/2^-_1$	271	300(8)
		^{221}Fr	
E1	$3/2^+_0 \to 1/2^-_0$	4.4^{-4}	5.3×10^{-4} (12)
E1	$7/2^+_0 \to 5/2^-_0$	2.3×10^{-4}	3.8×10^{-4} (10)
E1	$7/2^+_0 \to 9/2^-_0$	5.8×10^{-4}	4.1×10^{-4} (11)
E2	$3/2^-_0 \to 5/2^-_0$	23	23 (16)

Table 1, *continued*

Mult	Transition	Th [W.u.]	Exp [W.u.]
E2	$3/2_0^- \rightarrow 5/2_0^-$	23	23 (16)
E2	$7/2_0^- \rightarrow 3/2_0^-$	320	320 (12)
E2	$7/2_0^- \rightarrow 5/2_0^-$	2	16 (8)
E2	$7/2_0^- \rightarrow 9/2_0^-$	3	13
E1	$3/2_1^+ \rightarrow 3/2_1^-$	1.5×10^{-4}	3.8×10^{-4} (11)
E1	$3/2_1^+ \rightarrow 5/2_1^-$	0.3×10^{-4}	2.1×10^{-4} (7)
E1	$5/2_1^+ \rightarrow 3/2_1^-$	0.9×10^{-4}	1.7×10^{-4}(12)
E1	$5/2_1^+ \rightarrow 5/2_1^-$	4×10^{-5}	3.4×10^{-5} (16)
E1	$5/2_1^+ \rightarrow 7/2_1^-$	2×10^{-7}	2.6×10^{-4} (13)
E2	$7/2_1^- \rightarrow 3/2_1^-$	57	55
		^{223}Ra	
E1	$3/2_0^- \rightarrow 5/2_0^+$	2.8×10^{-4}	5.0×10^{-4} (9)
E1	$7/2_0^- \rightarrow 5/2_0^+$	2.33×10^{-4}	0.79×10^{-4}(24)
E1	$3/2_0^- \rightarrow 3/2_0^+$	3×10^{-5}	119×10^{-5} (16)
E1	$7/2_0^- \rightarrow 7/2_0^+$	9×10^{-6}	20×10^{-6} (22,-5)
E1	$3/2_2^- \rightarrow 1/2_2^+$	3.35×10^{-4}	1.60×10^{-4} (20)
E2	$7/2_0^- \rightarrow 3/2_0^-$	15	10 (6)
E2	$7/2_0^+ \rightarrow 5/2_0^+$	18	70
E2	$7/2_0^+ \rightarrow 3/2_0^+$	150	44
E2	$11/2_0^+ \rightarrow 7/2_0^+$	207	280 (12)
		^{239}Pu	
E1	$7/2_1^- \rightarrow 7/2_1^+$	1.28×10^{-7}	1.28×10^{-7} (20)
E2	$5/2_0^+ \rightarrow 3/2_0^+$	90	220 (5)
E2	$5/2_0^+ \rightarrow 1/2_0^+$	312	291 (47)
E2	$9/2_0^+ \rightarrow 7/2_0^+$	27	27 (20)
E2	$9/2_0^+ \rightarrow 5/2_0^+$	450	440 (4)

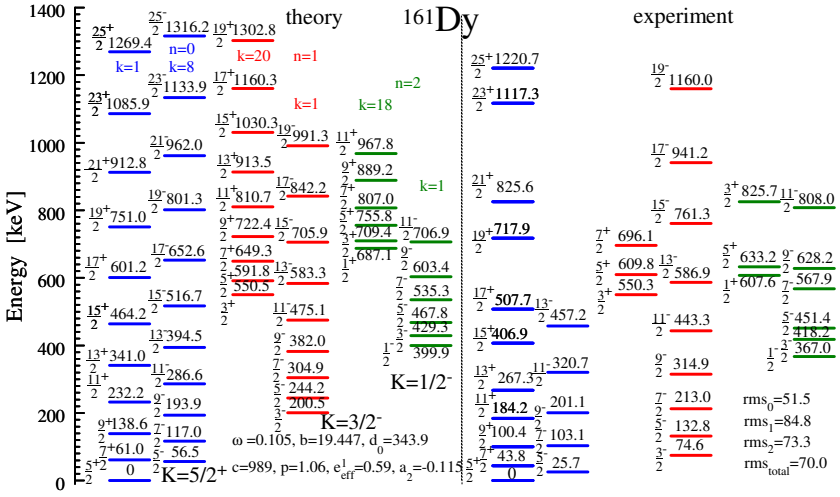

Figure 2. The same as Figure 1, but for ^{161}Dy.

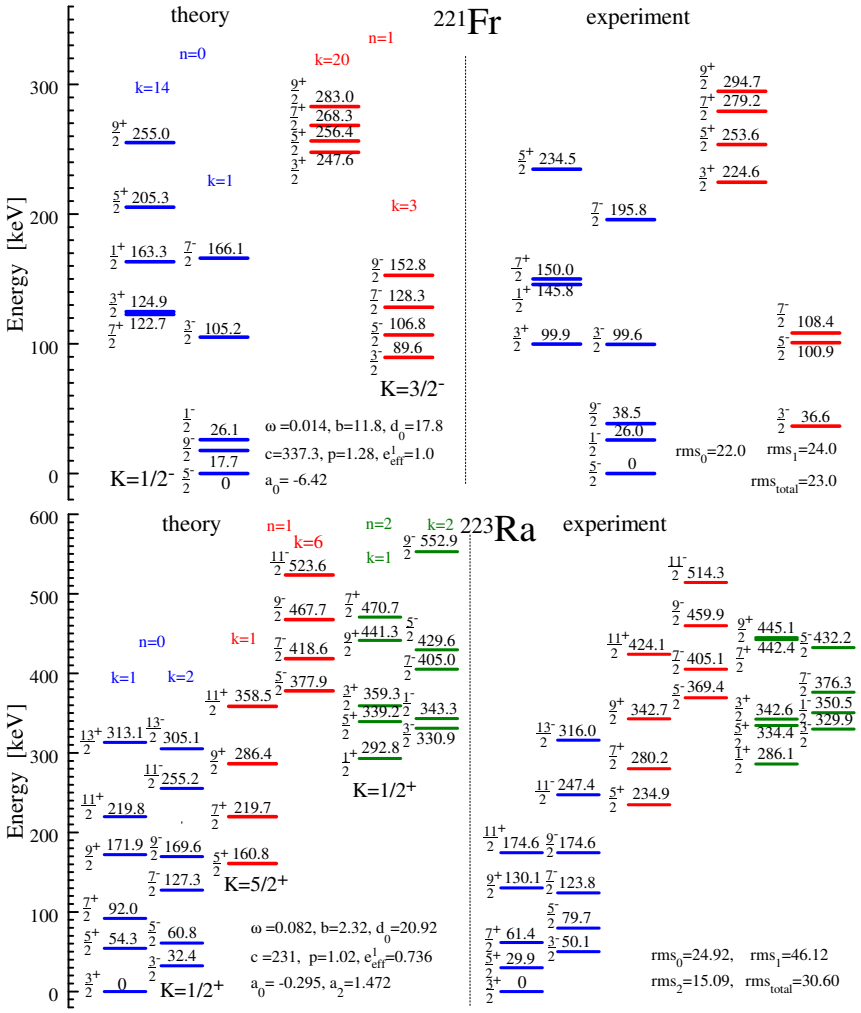

Figure 3. The same as Figure 1, but for ^{221}Fr and ^{223}Ra.

parameters are given in Figure 3. Also, we remark that in ^{223}Ra the yrast band is described by imposing $K = 1/2^+$ instead of the experimentally suggested $K = 3/2^+$. This is motivated by the previously indicated staggering behaviour of the doublet splitting which is considered as the manifestation of a Coriolis decoupling effect in that band [4].

The values of the quantum number k obtained for the different energy sequences of each nucleus (shown in Figures 1-4) carry information about their mutual disposition. The root mean square (rms) deviation between the theory and experiment obtained for the different sequences as well as the total rms fac-

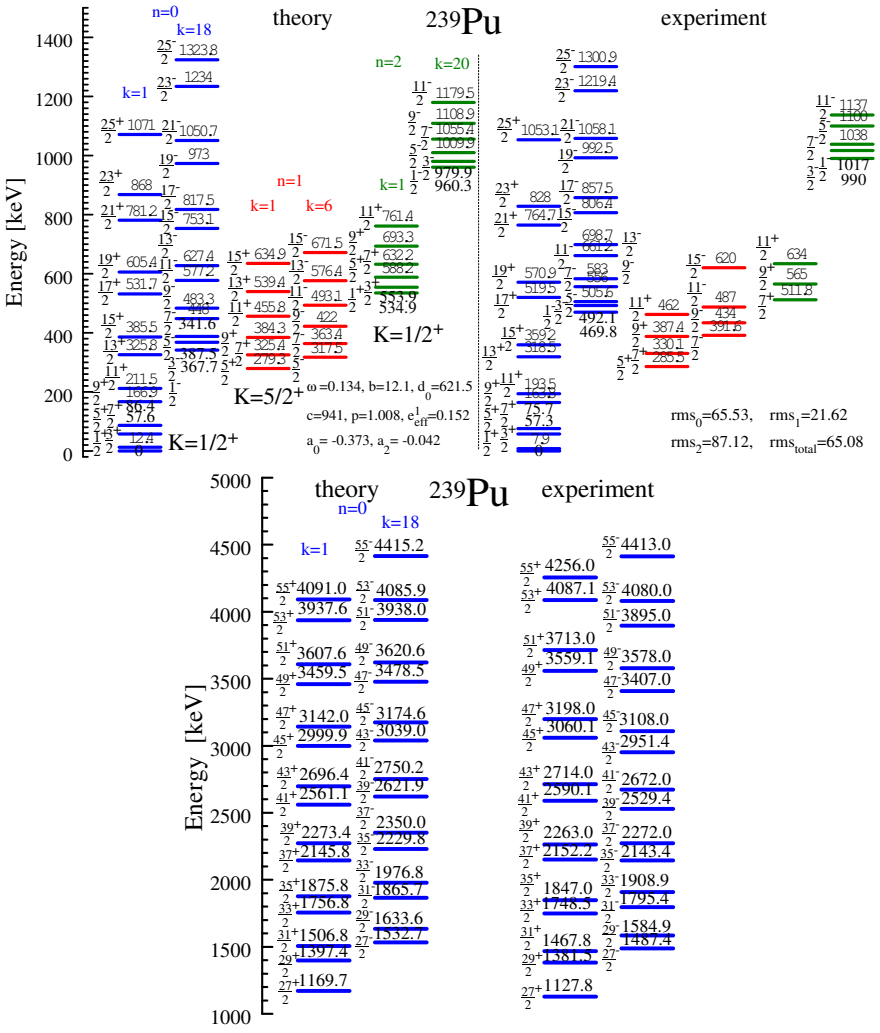

Figure 4. The same as Figure 1, but for ^{239}Pu. The lower panel contains the higher-spin part of the spectrum. Data from [7] and [9].

tor in the considered nuclei show the good quality of the model description. We especially remark the good model description of the energy levels and the B(E1) and B(E2) transition probabilities in the nuclei ^{239}Np and ^{243}Am, with energy rms factors 11.8 keV and 17.2 keV, respectively, shown in Figure 5. (Note the rms factor of 2.7 keV for the non-yrast states in ^{239}Np.)

The theoretical and experimental values of the B(E1) and B(E2) transition probabilities for the other nuclei are given in Table 1. They show an overall good

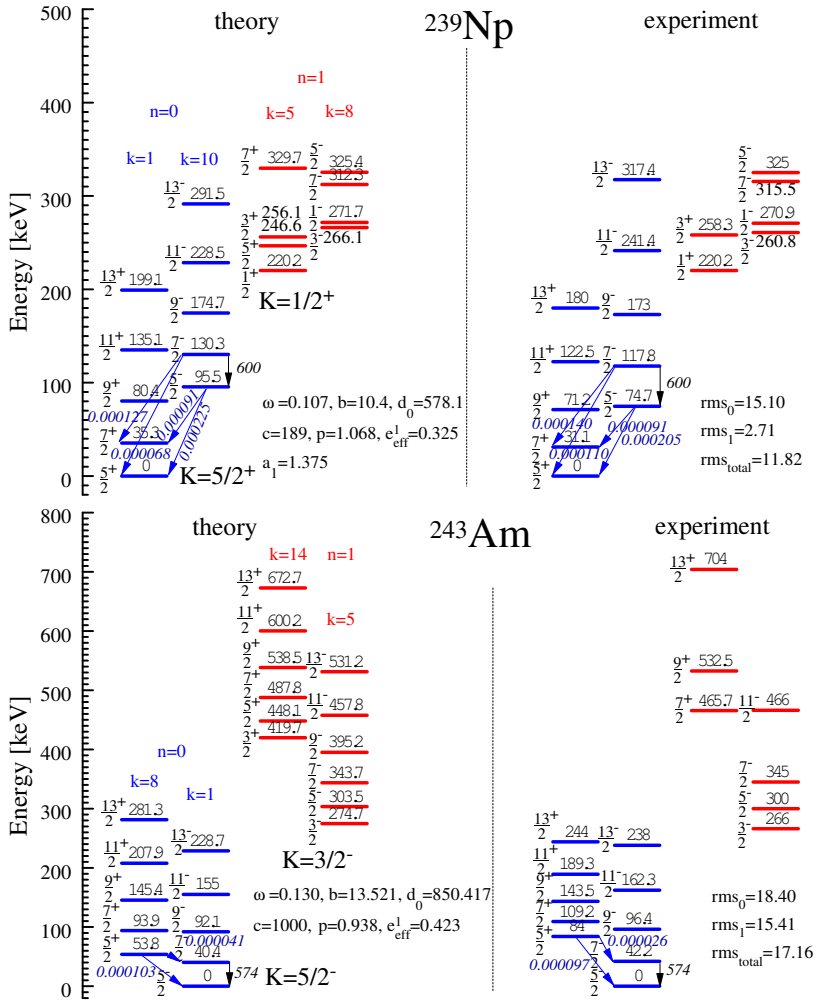

Figure 5. The same as Figure 1, but for ^{239}Np and ^{243}Am. The theoretical and experimental B(E1) and B(E2) transition probabilities are also given. Data from [8].

agreement between theory and experiment with few larger discrepancies being observed for some E1 transitions in the yrast bands of ^{221}Fr and ^{223}Ra. The latter can be explained with the more complicated structure due to the presence of the Coriolis interaction. In few cases where only one B(E1) or B(E2) value is described (*e.g.* in ^{239}Pu, ^{239}Np and ^{243}Am) we have an exact agreement between the theory and experiment due to the exact determination of the parameters c and p in the fitting procedure. In addition we should remind that transitions between states with different K-values are not included in the consideration.

The CQOM description of yrast and non-yrast quasi-doublet spectra of the odd-mass nuclei illustrated in Figures 1-5 shows that the model is capable to reproduce the specific spectroscopic properties related to the simultaneous manifestation of quadrupole and octupole degrees of freedom in these nuclei. It should be recognized that the successful descriptions are particularly due to the allowed jumps of the angular-oscillator quantum number k over several low-lying model states within the considered quasi-doublet structures. So far, this is only justified by the meaning of the differences in the k-values as characteristics of the mutual displacement of the opposite-parity sequences. The search for a deeper meaning and more sophisticated correlation between the quadrupole and octupole modes capable to compensate or explain these jumps is still an open issue. On the other hand even on the present level of phenomenology, the CQOM model description provides useful information for the initiation of further developments. As it was mentioned in the end of Sec. 2 the knowledge of the decoupling factors as well as the model mechanism for the forming of parity-doublet spectra in odd-mass nuclei can guide the inclusion of microscopic calculations in the study.

4 Conclusion

In conclusion, the present work provides an extended application of the collective model of Coherent Quadrupole and Octupole Motion (CQOM) for the description of yrast and non-yrast quasi-doublet spectra in odd-mass nuclei. The numerical results obtained for a number of odd mass nuclei in the rare-earth and actinide regions illustrate the capability of the model to reproduce the structure of yrast and non-yrast energy levels together with the attendant B(E1) and B(E2) transition probabilities. At the same time the observed Coriolis decoupling effects are phenomenologically taken into account. On this basis the present CQOM model descriptions can serve as a starting point for the application of a deeper collective+microscopic approach in the exploration of nuclear quadrupole-octupole collectivity. Work in this direction is in progress.

Acknowledgements

This work is supported by DFG and by the Bulgarian National Science Fund (contract DID-02/16-17.12.2009).

References

[1] P.A. Butler and W. Nazarewicz, *Rev. Mod. Phys.* **68** (1996) 349.

[2] J. M. Eisenberg and W. Greiner, *Nuclear Theory: Nuclear Models* (North-Holland, Amsterdam, 1987), third, revised and enlarged edition, Vol. I.

[3] N. Minkov, P. Yotov, S. Drenska, W. Scheid, D. Bonatsos, D. Lenis and D. Petrellis, *Phys. Rev. C* **73** (2006) 044315.

[4] N. Minkov, S. Drenska, P. Yotov, S. Lalkovski, D. Bonatsos and W. Scheid, *Phys. Rev. C* **76** (2007) 034324.

[5] N. Minkov, S. Drenska, M. Strecker, W. Scheid and H. Lenske, *Phys. Rev. C* **85** (2012) 034306.

[6] N. Minkov, S. Drenska, M. Strecker and W. Scheid, *J. Phys. G: Nucl. Part. Phys.* **37** (2010) 025103.

[7] http://www.nndc.bnl.gov/ensdf/.

[8] http://www.nndc.bnl.gov/nudat2/indx_adopted.jsp.

[9] S. Zhu et al., *Phys. Lett. B* **618**, (2005) 51.